coatings

MDPI

Article

SiO_2@TiO_2 Coating: Synthesis, Physical Characterization and Photocatalytic Evaluation

A. Rosales [1], A. Maury-Ramírez [2], R. Mejía-De Gutiérrez [3], C. Guzmán [1] and K. Esquivel [1,*]

[1] Graduate and Research Division, Engineering Faculty, Universidad Autónoma de Querétaro, Cerro de las Campanas, Santiago de Querétaro 76010, Mexico; alicia.ros.perez@hotmail.com (A.R.); cgm1909@hotmail.com (C.G.)

[2] Civil and Industrial Engineering Department, Engineering Faculty, Pontificia Universidad Javeriana Cali, calle 18 #118-250, Cali 760031, Colombia; anibal.maury@javerianacali.edu.co

[3] Group of Composite Materials, School of Materials, Faculty of Engineering, Universidad del Valle, Calle 13 #100-00, Cali 76001, Colombia; ruby.mejia@correounivalle.edu.co

* Correspondence: karen.esquivel@uaq.mx; Tel.: +52-442-192-12-00 (ext. 65401)

Received: 2 February 2018; Accepted: 19 March 2018; Published: 24 March 2018

Abstract: Use of silicon dioxide (SiO_2) and titanium dioxide (TiO_2) have been widely investigated individually in coatings technology, but their combined properties promote compatibility for different innovative applications. For example, the photocatalytic properties of TiO_2 coatings, when exposed to UV light, have interesting environmental applications, such as air purification, self-cleaning and antibacterial properties. However, as reported in different pilot projects, serious durability problems, associated with the adhesion between the substrate and TiO_2, have been evidenced. Thus, the aim of this work is to synthesize SiO_2 together with TiO_2 to increase the durability of the photocatalytic coating without affecting its photocatalytic potential. Therefore, synthesis using sonochemistry, synthesis without sonochemistry, physical characterization, photocatalytic evaluation, and durability of the SiO_2, SiO_2@TiO_2 and TiO_2 coatings are presented. Results indicate that using SiO_2 improved the durability of the TiO_2 coating without affecting its photocatalytic properties. Thus, this novel SiO_2@TiO_2 coating shows potential for developing long-lasting, self-cleaning and air-purifying construction materials.

Keywords: hydrophobic; photocatalytic; sonochemistry; coating; mortar

1. Introduction

Current environmental problems observed in big cities, such as air pollution and associated infrastructure deterioration, encourage research for the development of new technologies and products that mitigate these modern, urban threats. Among the different environmentally-friendly technologies, heterogeneous photocatalytic oxidation using TiO_2 has become an interesting technology due to its durability and high photocatalytic activity [1]. Recently, the incorporation of TiO_2 (e.g., coatings or additives) into construction materials used in urban infrastructure, such as concrete and mortars, has been an interesting approach to reduce NO_x and VOCs (volatile organic compounds) at outdoor concentrations using sunlight as the only energy source; these are the so-called air purifying properties. TiO_2 under UV-A light irradiation can generate oxidative (·OH) and reductive (·O_2) species, which are able to degrade different organic and inorganic compounds [2–4]. Furthermore, exposure to UV-A light enhances the superhydrophilic effect on the TiO_2 surface, which makes it easier to remove the fouling substances on TiO_2 loaded surfaces; this is the so-called self-cleaning ability [5–7]. However, recent applications of photocatalytic building materials in urban pilot projects have demonstrated that maintaining the durability of the air-purifying and self-cleaning properties remains challenging,

especially for the application of photocatalytic building materials under outdoor conditions [6]. Among other environmental factors, dust and oil accumulation have been reported as major factors affecting the properties of photocatalytic construction materials at an urban scale [7].

On the other hand, hydrophobic surfaces have also received attention for their self-cleaning, anti-flogging, anti-adherent and anti-polluting properties. The natural model for the design of superhydrophobic synthetic films is the lotus plant, which is known for its self-cleaning properties that allow the capture of air under water droplets that contribute to the rolling water droplet, a characteristic of well-designed superhydrophobic surfaces [8]. Due to the nano-manufacturing technologies that have been established for silicon substrates, silicon has been widely used for producing superhydrophobic surfaces; moreover, this kind surfaces, for instance, promotes durability in structures by avoiding the incrustation of corrosive salts (Cl^- and SO_4^-) that promote cracking or surface erosion [9]. To make superhydrophobic surfaces of intrinsically hydrophilic materials, a two-step process is usually required, i.e., first, make a rough surface and second, modify it with a coating of chemicals, such as organosilane, which may offer low surface energy after binding to the rough surface [9,10]. This is the case for polydimethylsiloxane (PDMS), which can be easily processed to make a hydrophobic surface with a rough texture and reduced free surface energy [11,12]. The methods to create hydrophobic surfaces have very long reaction times and strict chemical conditions. A method that uses sonochemistry has smaller reaction times, is more likely to undergo a complete chemical reaction and more ordered crystallization. Sonochemistry is a process of cavitation that refers to the rapid growth and collapse of implosion bubbles in a liquid in an unusual reaction environment [13,14]. Therefore, this article reports the development of a SiO_2@TiO_2 coating applicable to cement based materials, such as mortars and glass. The SiO_2 matrix, based on PDMS (polydimethylsiloxane), has the potential to increase the adherence of TiO_2 particles and to improve their photocatalytic efficiency [15].

2. Materials and Methods

As a strategy to develop an efficient SiO_2@TiO_2 coating, pure TiO_2 and pure SiO_2 coatings that used the same precursors, proportions, and two different synthesis methods were evaluated.

2.1. Synthesis of SiO_2@TiO_2 Coating Coupled with Sonochemistry

For TiO_2 sol production, titanium Iso-propoxide (97%, Sigma Aldrich, St. Louis, MO, USA) was added dropwise into an organic solvent (isopropyl alcohol, 99%, Sigma Aldrich), previously stirred under an inert nitrogen atmosphere for 5 min.

For SiO_2 synthesis, sonotrode equipment (Hielscher Ultrasound Technology UP200Ht, Teltow, Germany) was used working at 100% cavitation and 20% amplitude. A solution of distillated water, absolute ethyl alcohol and oxalic acid, in a 5/5/0.1 molar relation was prepared and stirred sonochemically for 15 min. Afterwards, tetraethyl orthosilicate was added dropwise and the mixture was stirred sonochemically for 3 min. Next, polydimethylsiloxane was added dropwise and continuously stirred for 3 min.

Finally, the titanium dioxide sol and the silicon dioxide sol were mixed. Beforehand, sonotrode working conditions were modified from the initial conditions to 100% cavitation and 60% amplitude. Immediately after mixing, 10 mL of distilled water was added and mixed continuously using sonotrode conditions for 20 min. The resultant mixture was applied on glass and mortar surfaces and left to dry at room temperature.

Synthesis of SiO_2@TiO_2 Coating without Sonochemistry

For TiO_2 sol preparation, after sol formation, a hydrolysis process was carried out with the addition of distilled water, added dropwise. The resulting solution was filtered, washed with distilled water and dried at room temperature for 18 h. Finally, a calcination process was carried out at 450 °C for 3 h.

For SiO_2, a solution of distillated water, absolute ethyl alcohol and oxalic acid, in a 5/5/0.1 molar relation was prepared and stirred for 15 min. Afterwards, tetraethyl orthosilicate was added dropwise and stirred for 3 min. Then, polydimethylsiloxane was added dropwise and stirred continuously for 3 min.

Finally, the titanium dioxide particles and the silicon dioxide sol were mixed for 20 min. The resultant mixture was applied on mortar surfaces and dried at room temperature for at least 1 h.

2.2. Preparation of Mortar Samples

The mortar samples were manufactured using a previous mix design (Table 1), the same local materials, and the ASTM method C192/C192M [16–18].

Table 1. Mortar components and proportions for 1 m^3.

Material	Proportions Related to Cement Content	Mass (kg)	Absolute Volume (dm^3)
Water	0.59	324.00	324.00
Cement	1.00	549.00	186.70
Aggregate	2.66	1421.40	489.30

2.3. Physical Characterization of SiO_2@TiO_2 Coating

The microstructures of the materials were examined by transmission electron microscopy (TEM) using a JEOL JEM-1010 (Tokyo, Japan), operating at a voltage of 200 kV. The crystallinity of the SiO_2@TiO_2 coating was determined by X-ray diffraction (XRD) using Bruker D8 equipment (Billerica, MA, USA) with a sealed copper tube to generate Cu–Kα radiation (λ = 1.15406 Å) with angles of $10 < 2\theta < 80°$ in a pitch of 0.01°. To verify the crystallinity, the structures of the obtained samples were characterized using Raman spectroscopy with the LabRAM HR equipment (Horiba Scientific, Kyoto, Japan), which used an NdYGA laser (λ = 532 nm). The samples were analyzed using a microscope with an objective of 10× at a power of 6 mW over a circle 1.5 μm in diameter. The optical transmittance of the glass substrates coated with SiO_2@TiO_2 was measured with a Cary 5000 UltraViolet-Visibe-Near-Infra-Red spectrophotometer (Agilent, Santa Clara, CA, USA) at wavelengths ranging from 350 to 800 nm. Water contact angle was measured using an optical tensiometer (Analyzer-DSA100W Krüss, Hamburg, Germany), which produces water droplets with a volume adjusted to 10 μL using a needle (stainless steel, model NE60).

2.4. Photocatalytic Evaluation

2.4.1. Evaluation of Photocatalytic Properties

The photocatalytic performance of the coating was evaluated using the method (UNI 11259-2016) based on Rhodamine B (RhB) degradation on the sample exposed to UV-A irradiation [19,20]. To monitor dye removal, the mortar samples were divided into three parts, in which TiO_2, SiO_2 and SiO_2@TiO_2 coatings were applied, as shown in Figure 1. Using a pipette, an RhB solution with a concentration of 50 ppm was evenly applied to 3 standardized positions on the samples, and they were left to dry overnight.

Then, the dye-contaminated samples were exposed to UV-A irradiation for 26 h using the UV reactor shown in Figure 2. In this reactor, UV-A irradiation was provided by an Electrolux T8 20 W/BLB. This lamp type emits light with a peak wavelength of 360 nm and an intensity of 10.3 $W \cdot m^{-2}$ at a distance of 5 mm. Finally, changes in color at 0, 4, and 26 h were measured using a portable X-rite Ci60 spectrophotometer (Photometric Solutions International, Victoria, Australia). Measurements were reported in the L^*, a^*, b^* colorimetric coordinates of the CIE LAB system (32/64 bit software), which corresponds to the white and black color range, red and green color range and yellow and blue color range, respectively, where the a^* coordinate is the comparison parameter. Based on these

measurements, the following parameters were calculated, as shown in Equations (1) and (2). Where R stands for color removal at time 0, 4, and 26 h of UV light exposition.

$$R_4 = \frac{(R_4 - R_0)}{R_0} \times 100 \quad (1)$$

$$R_{26} = \frac{(R_{26} - R_0)}{R_0} \times 100 \quad (2)$$

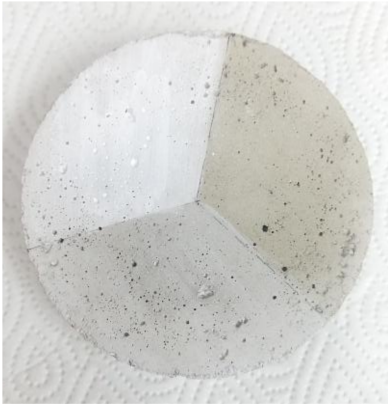

Figure 1. Mortar surface coated with TiO_2, SiO_2 and SiO_2@TiO_2 coatings.

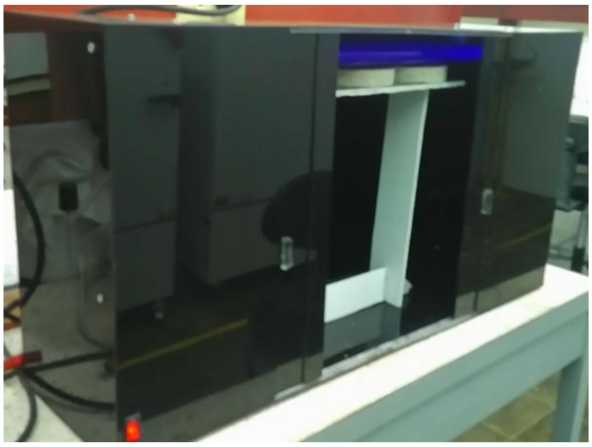

Figure 2. UV-A reactor using Electrolux T8 20W/BLB, λ = 360 nm, intensity = 10.3 W·m^{-2}.

2.4.2. Water Contact Angle Measurements

To evaluate the water behavior on the TiO_2, SiO_2 and SiO_2@TiO_2 coated samples, a preliminary test using the "rising drop" method was employed, using a camera and digital measurements, before and after the UV A light exposure (0, 4, and 26 h).

2.5. Durability

To assess the durability of the SiO_2, TiO_2 and SiO_2@TiO_2 coated samples, an adherence test was performed following the ASTM 3359 [21] and the appropriate references [22–27]. In this case, the corresponding test for thin films with thicknesses less than or equal to 2 mm was selected. To perform this test, a grid of 1 mm × 1 mm with eleven cuts of $\frac{3}{4}$ (20 mm) in length was drawn on top of the coated mortar sample. Subsequently, a piece of scotch tape, three inches long, was placed in the center of the grid and soft pressed with an eraser. A change in color of the tape indicated complete

contact. Then, the scotch tape was removed from the opposite end of the application, forming a 180° angle. Next, the coated area was compared with the patterns presented in Table 2 [22–25]. In addition, the adherence test was carried out before and after UV light exposure (0, 4 and 26 h), to determine the photocatalytic activity of the SiO_2@TiO_2 coating.

Table 2. Detachment patterns and classification of different coated surfaces after the adherence test (Modified from ASTM-3359-02 classification chart).

Classification	Area Removed (%)	Cross-Cut Surface Area with Adhesion Range by Percent
5B	None 0%	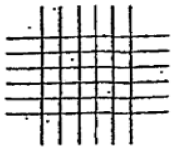
4B	<5%	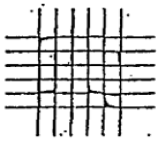
3B	5–15%	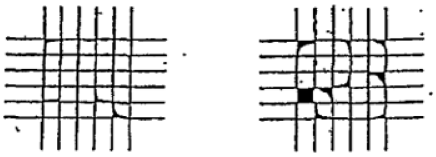
2B	15–35%	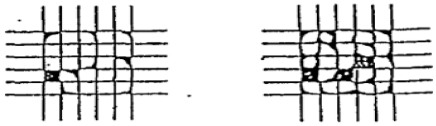
1B	35–65%	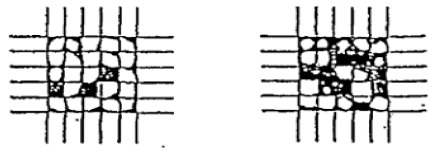
0B	>65%	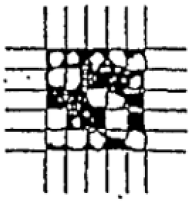

3. Results and Discussion

3.1. Physical Characteristics

TEM images (10×) of a power sample from the SiO_2@TiO_2 coating are shown in Figure 3. From these, it can be seen that layered agglomerates are formed by amorphous silicon dioxide while titanium dioxide is not visible. In general, the reported agglomerates vary in shape and size, ranging from 20–600 nm. In addition, it was observed that the morphology of the SiO_2@TiO_2 coating was not affected by the use of sonochemistry.

Figure 4 shows the SEM micrographs of the SiO_2@TiO_2 coating. It can be observed that the surface was rugged and the morphology was not uniform due to the formation of denser particles and

their agglomeration. Additional cross-selection elemental mappings, combined with EDS analysis for SiO_2@TiO_2, showed the presence of Si, Ti and O as elements (Figure 5) as expected.

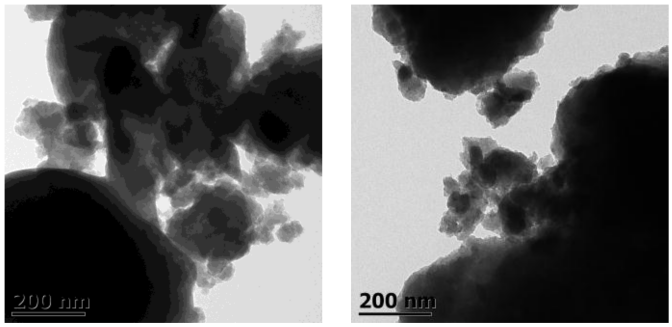

Figure 3. TEM images of the SiO_2@TiO_2 powder sample (10×).

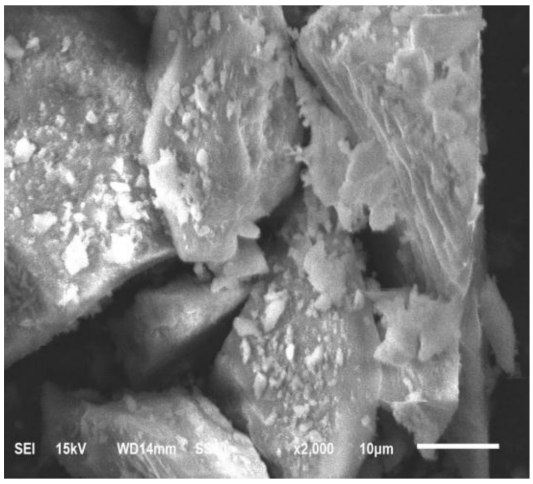

Figure 4. SEM micrographs of the SiO_2@TiO_2 coating in a power sample.

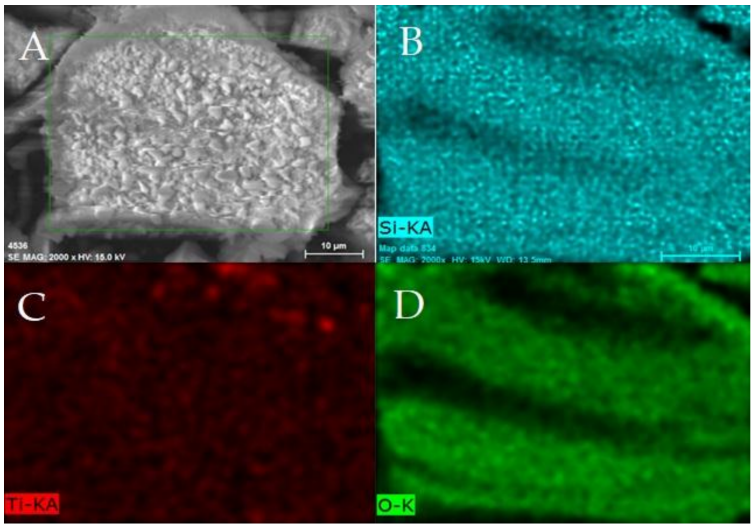

Figure 5. EDS analysis, elemental mapping images of the SiO_2@TiO_2 power sample: (**A**) EDS area; (**B**) Silicon; (**C**) Titanium and (**D**) Oxygen.

Figure 6 shows an X-ray diffractogram of the SiO_2@TiO_2 coating. It shows the high intensity peak of silicon dioxide at 24°, characteristic of the amorphous SiO_2 phase. In addition, signals observed at 12.8° and 22.6° are characteristic of the PDMS compound. On the other hand, signals of titanium dioxide that presented at peaks of 27.3° (110) and 55.5° (220) corresponded to the rutile crystalline phase [24] and the peaks of 25.3° (101), 38.6° (004) and 48.08° (200) corresponded to the anatase crystalline phase [25]. Additionally, it was observed that the diffractogram of the SiO_2@TiO_2 coating was not affected by the use of sonochemistry on a macro scale. Previous information was obtained using the standard XRD pattern (JCPDS FILES No. 21-1272). Moreover, the reflections corresponding to the silicon covered up the other signals of the TiO_2 phases and PDMS compound. The crystallite size was obtained by Scherrer's equation [26], which obtained a crystal size of 13 nm, being an amorphous compound due to its matrix of silicon dioxide.

The Raman spectra of TiO_2, SiO_2, SiO_2-PDMS and SiO_2@TiO_2 are presented in Figure 7. The Raman spectrum of TiO_2 contained a strong peak at 143 cm^{-1} and weak peaks at 395 cm^{-1}, 515 cm^{-1} and 638 cm^{-1}. The Raman spectrum of SiO_2 contained a strong peak at 450 cm^{-1} and weak peaks at 80 cm^{-1}, 90 cm^{-1} and 980 cm^{-1}. These peaks can be attributed to the bending of O–Si–O and Si–O–Si symmetric bond stretching. The Raman spectrum of SiO_2-PDMS exhibited peaks at 680 cm^{-1}, 816.1 cm^{-1}, 830.1 cm^{-1} and 882.4 cm^{-1}, these peaks are characteristic of the PDMS compound [27].

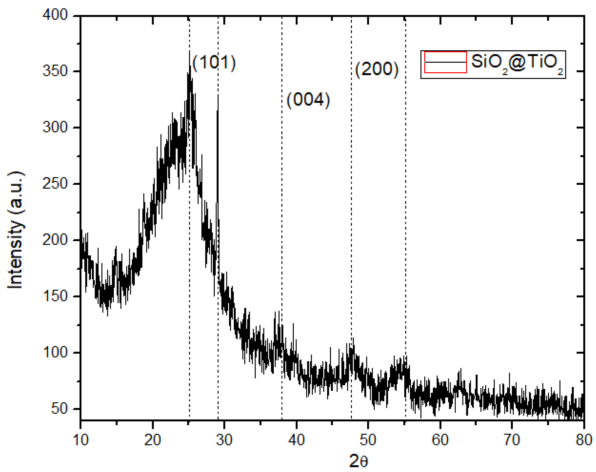

Figure 6. XRD pattern of the SiO_2@TiO_2 coating.

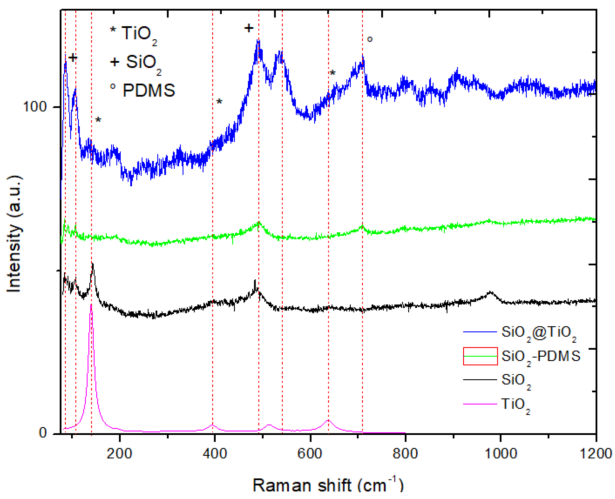

Figure 7. Raman spectra in the range of 80–1200 cm^{-1} from TiO_2, SiO_2 and SiO_2@TiO_2.

The Raman spectrum of the SiO_2@TiO_2 nanocomposite exhibited a decrease in the highest intensity peak of titanium dioxide while the other peaks were inhibited. This can be attributed to the highly dispersed titanium dioxide. Furthermore, the signals of silicon dioxide decreased due to the presence of PDMS that modifies the crystallinity and makes noise (fluorescence) on the SiO_2@TiO_2 coating. The Raman spectrum of the SiO_2@TiO_2 coating, without the application of sonochemistry, showed a lower crystallinity for the composite. Furthermore, the TiO_2 signals were decreased and not even located by the Raman Spectroscopy.

Figure 8 shows the UV-visible spectrum of a glass sample coated with SiO_2@TiO_2 with reference to a blank (uncoated glass). The glass substrate had a transmittance of 92–93% (black line). After placing the coating on the glass, the transmittance of sample (blue line) was 85%. This result shows that the coating of SiO_2@TiO_2 has high transparency over a wide wavelength range.

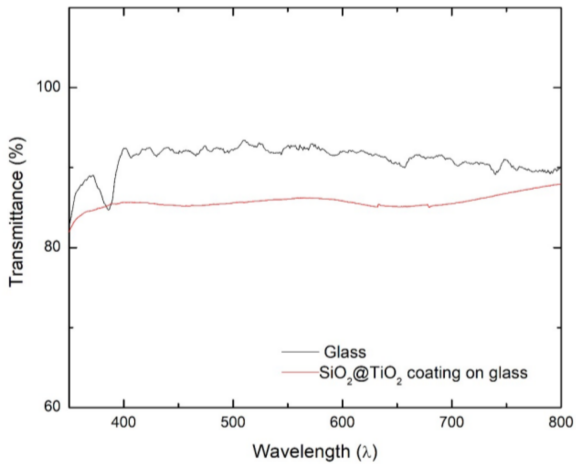

Figure 8. UV-Vis transmittance spectra of SiO_2@TiO_2 coated on glass (red) and glass (black).

3.2. Photocatalytic Evaluation

By measuring the RhB degradation before (0 h) and after UV-A irradiation (4 and 26 h) as shown in Figure 9, the TiO_2, SiO_2 and SiO_2@TiO_2 coated mortar samples were evaluated (Figure 10). With RhB removal of R_4 = 25% and R_{26} = 55%, the developed SiO_2@TiO_2 coating satisfies the boundaries as to what can be considered photocatalytic material (R_4 > 20% and R_{26} > 50%) [19]. However, the use of sonochemistry showed an improvement in the efficiencies of degradations of R_4 = 30.4% and R_{26} = 70.5%. Similar values have been also reported by a photocatalytic coating applied on mortar samples [28].

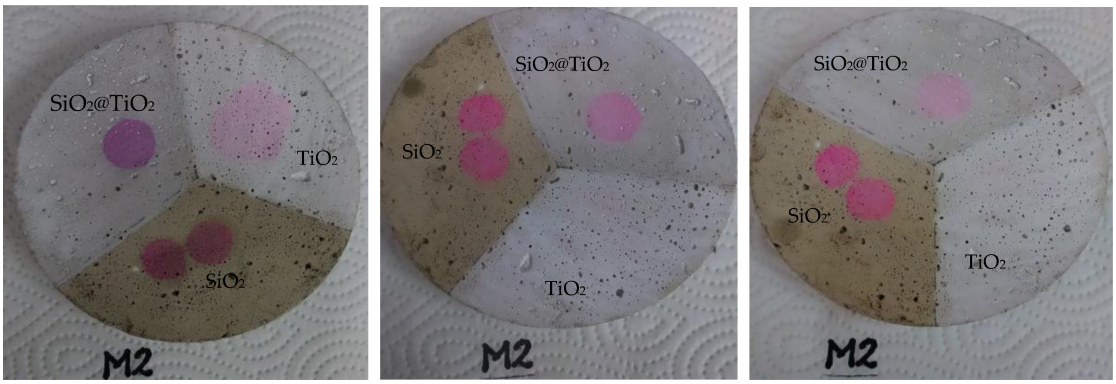

(**a**) (**b**) (**c**)

Figure 9. Comparison of the degradation of RhB, before and after UV-A irradiation. (**a**) 0 h; (**b**) 4 h; (**c**) 26 h.

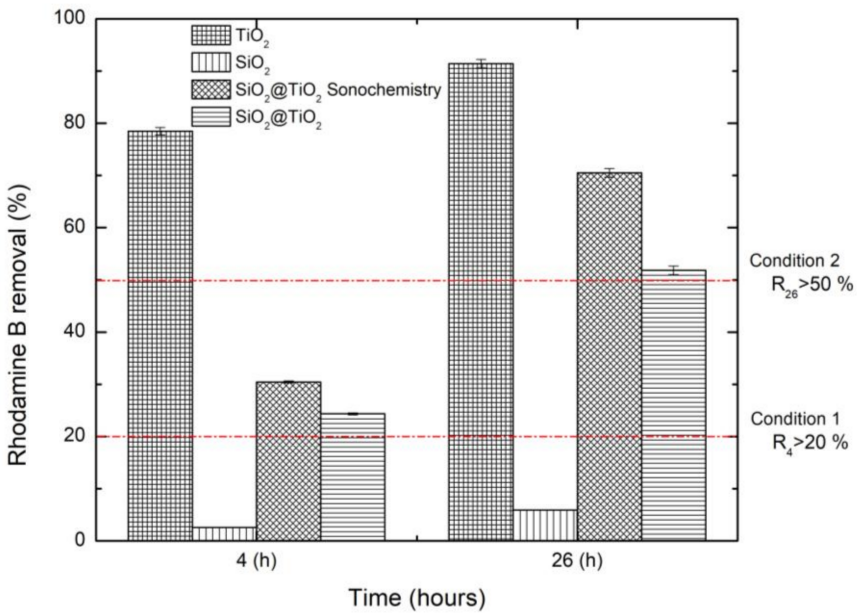

Figure 10. Rhodamine B removal efficiencies of the TiO_2, SiO_2 and SiO_2@TiO_2 coated mortar samples under UV-A irradiation (4 and 26 h).

On the other hand, as expected, TiO_2 coated samples displayed the best activity with R_4 = 79% and R_{26} = 92% [29]. In contrast, the SiO_2 coated samples exhibited a significantly lower degradation efficiency (R_4 = 0.5%, R_{26} = 8%). As there was no photocatalytic material present, the RhB removal was associated with dye photolysis, as previously reported [30]. According to the physico-chemical characterization of the SiO_2@TiO_2 composite previously described, the synthesis coupled with sonochemistry showed a non-significant difference in performance. Nevertheless, in the photocatalytic activity, the use of the sonochemical assisted synthesis helped to improve the Rhodamine B removal. This could be attributed to a better TiO_2 dispersion over the SiO_2-PDMS matrix and a higher anatase phase appearance without any thermal treatment as is used with the conventional sol-gel SiO_2@TiO_2 composite synthesis. However, this effect must be examined in further experiments by an extensive XPS analysis and by modifying the sonochemical synthesis parameters to achieve a macroscopic change in the physico-chemical characterization.

The water contact angle measurements of TiO_2, SiO_2 and SiO_2@TiO_2 coated mortar samples before, during and after UV irradiation (0, 4 and 26 h) are shown in Figure 11. As expected, TiO_2 exhibited hydrophilic behavior with values around 10°. On the contrary, the coated sample with SiO_2@TiO_2 presented water contact angles varying between 100° and 105° after UV-A irradiation. Previous research reports similar contact angles of around 114°–111° for a coating of TiO_2-SiO_2-PDMS [31]. Meanwhile the SiO_2 coated samples remained constant (around 98°) because silicon dioxide has hydrophobic properties.

Table 3 shows the adherence test results of the coated mortar samples using TiO_2, SiO_2 and SiO_2@TiO_2. In the case of the SiO_2@TiO_2, a 10% detachment was quantified using the grid which classifies as 3B according to the ASTM D3359-02 [22,32]. On the other hand, the TiO_2 presented with 40% detachment, which classifies as 1B. Finally, SiO_2 had the highest adherence of the tested coatings and presented with 5% detachment and classifies as 4B.

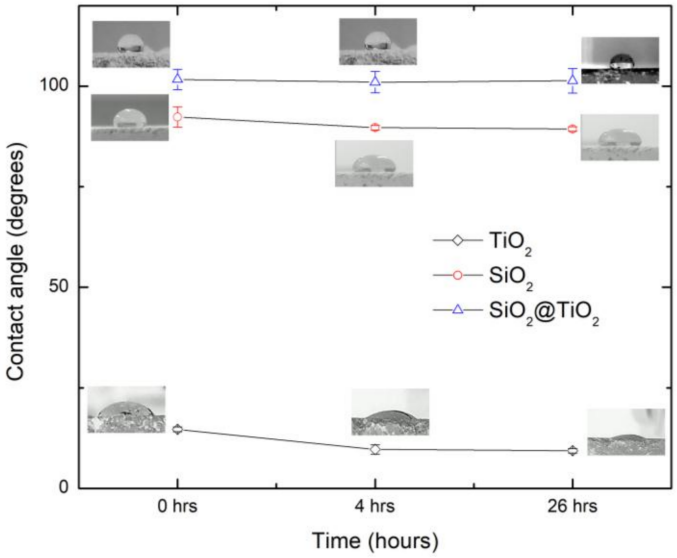

Figure 11. Water contact angles of TiO_2, SiO_2 and SiO_2@TiO_2 coated mortar samples before (0 h) and under UV-A irradiation (4 and 26 h).

Table 3. Test of adherence results of the coated mortar samples using TiO_2, SiO_2 and SiO_2@TiO_2.

Coated Sample	% Detachment	Image	Classified under ASTM D3359-02
TiO_2	40%	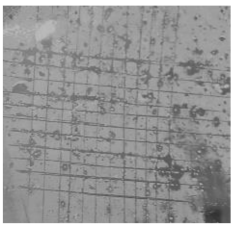	1B
SiO_2	5%	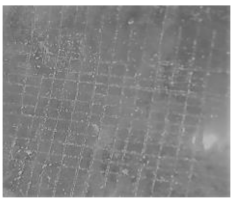	4B
SiO_2@TiO_2	10%		3B

After the evaluation of durability using the adherence test, Rhodamine B removal and water contact angle measurements were evaluated again on the coated samples. Results indicated that TiO_2 decreased its photocatalytic activity to R_4 = 44% and R_{26} = 70%. For the SiO_2@TiO_2 coating no difference was noticed, while SiO_2 did not show a change in its photocatalytic activity. The contact angle was also maintained for all the tested materials. The results were 5° for the TiO_2 90° SiO_2 and 100° SiO_2@TiO_2. Further experiments will be needed to find out the effects of extreme weather conditions on the durability of the coat.

4. Conclusions

In the present study, a hydrophobic and photocatalytic SiO_2@TiO_2 coating for mortar and glass protection was synthesized through a sol-gel with and without sonochemistry assistance. The completed analysis of Scanning Microscopy (SEM), Elemental Analysis (EDS), Transmission Electron Microscopy (TEM), X-ray diffraction (XRD) and Raman Spectroscopy of the SiO_2@TiO_2 coating revealed their composition and microstructure. The TEM images made it possible to observe agglomerates of the composite without a regular shape. But, by mapping the EDS analysis the main elements were found over the entire surface in a homogeneous way. The use of XRD enabled the visualization of the TiO_2 phases formed using sonochemistry. These phases are the rutile and anatase phase. Additionally the SiO_2 remained amorphous. Further, the Raman spectroscopy signals can be attributed to the bending and stretching of the O–Si–O and Si–O–Si symmetric bonds and without the application of sonochemistry a lower crystallinity of the composite and the TiO_2 signals was observed. Finally, according to the physico-chemical characterization of SiO_2@TiO_2, the coating displayed a high transparency over a wide wavelength range.

In addition, the application of sonochemistry in the sol-gel synthesis promoted the photocatalytic phase of the titanium dioxide and improved the removal of the Rhodamine B dye. The transparency of the titanium dioxide coating was around 85% of that compared to glass without a cover.

The photocatalytic activity of the SiO_2@TiO_2 coating showed an RhB removal of R_4 = 25% and R_{26} = 55% establishing itself as a photocatalytic material, while the SiO_2@TiO_2 coating coupled with sonochemistry showed R_4 = 30.4% and R_{26} = 70.5% indicating a major photocatalytic activity. The adherence test was used to study the durability, indicating a 3B type adhesion of the SiO_2@TiO_2, in accordance with the ASTM D3359-02 scale. Additionally, the SiO_2@TiO_2 composite after the durability tests showed no photocatalytic activity loss in contrast with the pure TiO_2 coating. These results show the potential of the developed SiO_2@TiO_2 coating for self-cleaning and air-purifying applications.

Acknowledgments: A. Rosales thanks CONACyT for the scholarship granted and also thanks to UniValle and PUJ Cali for the facilities in the international mobility exchange. C. Guzmán and K. Esquivel thanks to Luis A. Ortiz-Frade from CIDETEQ for the SEM and EDS analysis, to QFB. Lourdes Palma from UNAM for the TEM images and to Luis Escobar-Alarcón from ININ for the Raman analysis.

Author Contributions: K. Esquivel and A. Maury-Ramírez conceived and designed the experiments; A. Rosales performed the experiments; all the authors analyzed the data; R. Mejía-De Gutiérrez and C. Guzmán contributed reagents/materials/analysis tools; A. Rosales, A. Maury-Ramírez and K. Esquivel wrote the paper.

Conflicts of Interest: The authors declare no conflict of interest.

References

1. Creelman, L.W.; Pešinová, V.; Cohen, Y.; Winer, A.M. Intermedia transfer factors for modeling the enviromental impact of air pollution from industrial sources. *J. Hazard. Mater.* **1994**, *37*, 15–25. [CrossRef]
2. Hoffmann, M.R.; Martin, S.T.; Choi, W.; Bahnemann, D.W. Environmental applications of semiconductor photocatalysis. *Chem. Rev.* **1995**, *95*, 69–96. [CrossRef]
3. Ghosh, P.K.; Jasra, R.V.; Shukla, D.B.; Bhatt, A.K.; Tayade, R.J. Photocatalytic Auto-Cleaning Process of Stains. U.S. Patent No. 8,343,282, 1 January 2013.
4. Miyauchi, M.; Kieda, N.; Hishita, S.; Mitsuhashi, T.; Nakajima, A.; Watanabe, T.; Hashimoto, K. Reversible wettability control of TiO_2 surface by light irradiation. *Surf. Sci.* **2002**, *511*, 401–407. [CrossRef]
5. Natarajan, K.; Natarajan, T.S.; Bajaj, H.C.; Tayade, R.J. Photocatalytic reactor based on UV-LED/TiO_2 coated quartz tube for degradation of dyes. *Chem. Eng. J.* **2011**, *178*, 40–49. [CrossRef]
6. Boonen, E.; Beeldens, A.; Dirkx, I.; Bams, V. Durability of cementitious photocatalytic building materials. *Catal. Today* **2017**, *287*, 196–202. [CrossRef]
7. Etxeberria, M.; Guo, M.-Z.; Maury-Ramirez, A.; Poon, C.S. Influence of dust and oil accumulation on effectiveness of photocatalytic concrete surfaces. *J. Environ. Eng.* **2017**, *143*, 04017040. [CrossRef]
8. Cheng, Y.-T.; Rodak, D.E. Is the lotus leaf superhydrophobic? *Appl. Phys. Lett.* **2005**, *86*, 144101. [CrossRef]

9. Wang, D.; Hou, P.; Zhang, L.; Yang, P.; Cheng, X. Photocatalytic and hydrophobic activity of cement-based materials from benzyl-terminated-TiO_2 spheres with core-shell structures. *Constr. Build. Mater.* **2017**, *148*, 176–183. [CrossRef]
10. Stanton, M.M.; Ducker, R.E.; MacDonald, J.C.; Lambert, C.R.; Grant McGimpsey, W. Super-hydrophobic, highly adhesive, polydimethylsiloxane (PDMS) surfaces. *J. Colloid Interface Sci.* **2012**, *367*, 502–508. [CrossRef] [PubMed]
11. Ma, M.; Hill, R.M. Superhydrophobic surfaces. *Curr. Opin. Colloid Interface Sci.* **2006**, *11*, 193–202. [CrossRef]
12. Swart, M.; Mallon, P.E. Hydrophobicity recovery of corona-modified superhydrophobic surfaces produced by the electrospinning of poly(methyl methacrylate)-graft-poly(dimethylsiloxane)hybrid copolymers. *Pure Appl. Chem.* **2009**, *81*, 495–511. [CrossRef]
13. Mettin, R.; Cairós, C.; Troia, A. Sonochemistry and bubble dynamics. *Ultrason. Sonochem.* **2015**, *25*, 24–30. [CrossRef] [PubMed]
14. Rae, J.; Ashokkumar, M.; Eulaerts, O.; von Sonntag, C.; Reisse, J.; Grieser, F. Estimation of ultrasound induced cavitation bubble temperatures in aqueous solutions. *Ultrason. Sonochem.* **2005**, *12*, 325–329. [CrossRef] [PubMed]
15. Sangchay, W. The self-cleaning and photocatalytic properties of TiO_2 doped with SnO_2 thin films preparation by sol-gel method. *Energy Procedia* **2016**, *89*, 170–176. [CrossRef]
16. Sánchez de Guzmán, D. *Concrete and Mortar Technology (Tecnología del Concreto y del Mortero)*; Pontificia Universidad Javeriana: Bogotá, Colombia, 2001.
17. Medina Medina, A.F.; Torres Rojas, D.F.; Meza Girón, G.; Villota Grisales, R.A. System Design to Generate air Purification and Self-Cleaning Surfaces of the Tunnel of Colombia Avenue (Cali). (Diseño de un Sistema Para Generar Purificación del aire y Auto-Limpieza en las Superficies del Tunel de la Avenida Colombia (Cali)). Ph.D. Thesis, Pontificia Universidad Javeriana, Cali, Colombia, 2016.
18. ASTM International. *ASTM C192/C192M-16a Standard Practice for Making and Curing Concrete Test Specimens in the Laboratory*; ASTM International: West Conshohocken, PA, USA, 2016.
19. SAI Global. *UNI 11259: 2016 Determination of the Photocatalytic Activity of Hidraulic Binders-Rodammina Test Method*; SAI Global: Rome, Italy, 2016.
20. Maury-Ramirez, A.; Demeestere, K.; De Belie, N. Photocatalytic activity of titanium dioxide nanoparticle coatings applied on autoclaved aerated concrete: Effect of weathering on coating physical characteristics and gaseous toluene removal. *J. Hazard. Mater.* **2012**, *211–212*, 218–225. [CrossRef] [PubMed]
21. ASTM International. *ASTM D3359-02 Standard Test Methods for Measuring Adhesion by Tape Test*; ASTM International: West Conshohocken, PA, USA, 2002.
22. Fufa, S.M.; Labonnote, N.; Frank, S.; Rüther, P.; Jelle, B.P. Durability evaluation of adhesive tapes for building applications. *Constr. Build. Mater.* **2018**, *161*, 528–538. [CrossRef]
23. Bishop, C.A. *Vacuum Deposition onto Webs, Films and Foils*, 3rd ed.; William Andrew Publishing: Boston, MA, USA, 2015; pp. 197–208.
24. Cheng, P.; Zheng, M.; Jin, Y.; Huang, Q.; Gu, M. Preparation and characterization of silica-doped titania photocatalyst through sol–gel method. *Mater. Lett.* **2003**, *57*, 2989–2994. [CrossRef]
25. Haider, A.J.; AL–Anbari, R.H.; Kadhim, G.R.; Salame, C.T. Exploring potential Environmental applications of TiO_2 Nanoparticles. *Energy Procedia* **2017**, *119*, 332–345. [CrossRef]
26. Maury-Ramirez, A.; Nikkanen, J.-P.; Honkanen, M.; Demeestere, K.; Levänen, E.; De Belie, N. TiO_2 coatings synthesized by liquid flame spray and low temperature sol–gel technologies on autoclaved aerated concrete for air-purifying purposes. *Mater. Charact.* **2014**, *87*, 74–85. [CrossRef]
27. Al-Asbahi, B.A. Influence of anatase titania nanoparticles content on optical and structural properties of amorphous silica. *Mater. Res. Bull.* **2017**, *89*, 286–291. [CrossRef]
28. Guo, M.-Z.; Maury-Ramirez, A.; Poon, C.S. Photocatalytic activities of titanium dioxide incorporated architectural mortars: Effects of weathering and activation light. *Build. Environ.* **2015**, *94*, 395–402. [CrossRef]
29. Hashimoto, K.; Irie, H.; Fujishima, A. TiO_2 Photocatalysis: A Historical Overview and Future Prospects. *Jpn. J. Appl. Phys.* **2005**, *44*, 8269. [CrossRef]
30. Allen, N.S.; Binkley, J.P.; Parsons, B.J.; Phillips, G.O.; Tennent, N.H. Light stability and flash photolysis of azo dyes in epoxy resins. *Dyes Pigments* **1984**, *5*, 209–223. [CrossRef]

31. Kapridaki, C.; Maravelaki-Kalaitzaki, P. TiO_2–SiO_2–PDMS nano-composite hydrophobic coating with self-cleaning properties for marble protection. *Prog. Org. Coat.* **2013**, *76*, 400–410. [CrossRef]
32. Castañeda, A.; Rivero, C.; Corvo, F. Evaluación de sistemas de protección contra la corrosión en la rehabilitación de estructuras construidas en sitios de elevada agresividad corrosiva en Cuba. *Rev. Constr.* **2012**, *11*, 49–61. [CrossRef]